Respiratory Physiology & Neurobiology 165 (2009) 28–39

Contents lists available at ScienceDirect

Respiratory Physiology & Neurobiology

journal homepage: www.elsevier.com/locate/resphysiol

Estimating the effect of lung collapse and pulmonary shunt on gas exchange during breath-hold diving: The Scholander and Kooyman legacy

A. Fahlman[a,d,*], S.K. Hooker[b], A. Olszowka[c], B.L. Bostrom[d], D.R. Jones[d]

[a] Global Diving Research, Ottawa, ON, Canada K2J 5E8
[b] Sea Mammal Research Unit, Gatty Marine Laboratory, University of St Andrews, St Andrews, Fife KY16 8LB, Scotland
[c] Department of Physiology and Biophysics, The University at Buffalo, Buffalo, NY 14144, USA
[d] Department of Zoology, The University of British Columbia, 6270 University Blvd., Vancouver, BC, Canada V6T 1Z4

ARTICLE INFO

Article history:
Accepted 26 September 2008

Keywords:
Mathematical modeling
Diving physiology
Decompression sickness
Marine mammal
Nitrogen
Oxygen

ABSTRACT

We developed a mathematical model to investigate the effect of lung compression and collapse (pulmonary shunt) on the uptake and removal of O_2, CO_2 and N_2 in blood and tissue of breath-hold diving mammals. We investigated the consequences of pressure (diving depth) and respiratory volume on pulmonary shunt and gas exchange as pressure compressed the alveoli. The model showed good agreement with previous studies of measured arterial O_2 tensions (Pa_{O_2}) from freely diving Weddell seals and measured arterial and venous N_2 tensions from captive elephant seals compressed in a hyperbaric chamber. Pulmonary compression resulted in a rapid spike in Pa_{O_2} and arterial CO_2 tension, followed by cyclical variation with a periodicity determined by $\dot{Q}_{tot}$. The model showed that changes in diving lung volume are an efficient behavioural means to adjust the extent of gas exchange with depth. Differing models of lung compression and collapse depth caused major differences in blood and tissue N_2 estimates. Our integrated modelling approach contradicted predictions from simple models, and emphasised the complex nature of physiological interactions between circulation, lung compression and gas exchange. Overall, our work suggests the need for caution in interpretation of previous model results based on assumed collapse depths and all-or-nothing lung collapse models.

1. Introduction

Scholander suggested that the flexible rib cage, the rigid dead space (bronchi and trachea), the bag shaped diaphragm and the venous network on the pericardium of breath-hold diving marine mammals were anatomical adaptations that would allow the air from the alveoli to empty into the dead space during a dive (Scholander, 1940). The depth, or pressure, where the alveoli completely collapsed would be determined by the relative volumes of the dead space and alveoli. Assuming that the dead space does not compress until the alveoli are collapsed, this depth can be predicted using Boyle's law as follows:

$$P_{amb_c} = (DV_L \cdot V_D^{-1}) \cdot P_{amb_s}^{-1} \quad (1)$$

where P_{amb_c} is the collapse pressure, DV_L the initial diving lung volume, V_D the volume of the dead space and P_{amb_s} the ambient pressure at the surface.

However, Eq. (1) is based on the assumption that the dead space does not collapse while experimentally it has been shown to compress at depths <50 m (Ridgway, 1968; Kooyman and Hammond, 1970). A recent study modelled the simultaneous compression of dead space and alveoli predicting that Eq. (1) underestimates the depth at which the lungs collapse and a model that accounted for concurrent collapse of both the upper and lower respiratory system showed that the depth of complete alveolar collapse is dependent on DV_L and in most cases does not occur until a depth well below 100 m (Bostrom et al., 2008).

Scholander proposed that with an increasing pressure, as the alveoli compressed, the gas diffusion rate would initially increase, reach a maximum and then decrease to zero upon alveolar collapse (Scholander, 1940). The increased diffusion rate early in the dive results from an increasing alveolar-venous partial pressure gradient as the ambient pressure increases. However, alveolar compression will reduce the surface area available for gas exchange and thicken the alveolar membrane, both causing a decrease in the diffusion rate. A proxy for measurement of diffusion rate, the pulmonary shunt, has been measured in harbour seals and California sea lions subjected to pressures up to 10 ATA in a hyperbaric chamber (90 m, Kooyman and Sinnett, 1982). Pulmonary shunt represents the amount of blood bypassing the lung

* Corresponding author. Tel.: +1 240 476 8431.
E-mail address: andreas_fahlman@yahoo.com (A. Fahlman).

1569-9048/$ – see front matter © 2008 Elsevier B.V. All rights reserved.
doi:10.1016/j.resp.2008.09.013

and not participating in gas exchange. The shunt varies between 0% and 100%, where 0% represents a fully inflated lung with perfect gas exchange and 100% represents termination of gas exchange. Results indicated that pulmonary shunt increased with pressure but varied with DV_L. At 90 m a 70% shunt was observed and it was predicted that complete collapse would not occur until a depth >150 m (Kooyman and Sinnett, 1982) which is significantly deeper than the 30 and 70 m that were predicted for lung collapse from measuring N_2 uptake and removal in the Weddell seal (Falke et al., 1985) and bottlenose dolphin, respectively (Ridgway and Howard, 1979). Bostrom et al. (2008) suggested that varying collapse depths found in different studies could be explained by assumptions used in predicting the effect of pressure on gas exchange. When N_2 uptake and removal (Ridgway and Howard, 1979; Falke et al., 1985) were used to indirectly estimate collapse depth, it was assumed that the rate of diffusion increased linearly with pressure until collapse, at which time gas exchange immediately ceased. This assumption was also used by other models attempting to estimate blood and tissue PN_2 levels in breath-hold diving mammals and birds (Fahlman et al., 2006, 2007; Zimmer and Tyack, 2007). The estimated blood and tissue PN_2s were used to determine if birds and mammals are ever at risk of decompression sickness (DCS), but with a better understanding of how lung compression and pulmonary shunt are manifested, this could be much improved.

In order to better understand how inert and metabolic gases are exchanged during breath-hold diving we therefore examine the potential error in estimated blood and tissue gas tensions caused by the previous assumption of a linearly increasing diffusion rate compared with a model incorporating a more realistic pressure dependent increase in pulmonary shunt. Since pulmonary shunt is affected both by pressure and lung volume, predictions will vary for species according to mass specific lung volumes and metabolic rates. We formulate a new physiological model in which diffusion rate (shunt) is affected by the compression of the respiratory system during diving. In addition to consideration of N_2 exchange (Fahlman et al., 2006, 2007), this model also incorporates exchange of O_2 and CO_2. This allows us to assess how changes in lung gas during diving, as well as those affected by pulmonary compression, may affect gas exchange.

2. Material and methods

2.1. Model

The model described in this paper combines the breath-hold diving model developed by Fahlman et al. (2006) with the lung compression model developed by Bostrom et al. (2008). Exchange, production and consumption of O_2 and CO_2 were incorporated in addition to accounting for exchange of N_2.

The body was partitioned into 5 compartments or stores; blood (Bl), brain (B), fat (F), muscle (M) and central circulation (CC). The central circulatory compartment included heart, kidney, liver and alimentary tract while the muscle compartment included muscle, skin, bone, connective tissue and all other tissues. This partitioning differs from our earlier work and leaves the fat compartment containing only adipose tissue (Fahlman et al., 2006).

The model was parameterised and tested for elephant and Weddell seals and so was based on published values available for these species when possible, and failing this, on published values for other phocid species (as detailed below).

2.2. Lung gas stores

Gas exchange occurred between lung and blood and between blood and each compartment (Fig. 1 in Fahlman et al., 2006). The O_2, CO_2 and N_2 stores in the lung consisted only of a gas phase and were assumed to be homogenous. We assumed that there was no diffusion resistance at the lung surface interface when an animal was breathing at the surface (Farhi, 1967). Thus, arterial blood tension of N_2 (Pa_{N_2}), O_2 (Pa_{O_2}) and CO_2 (Pa_{CO_2}) were assumed to be equal to the alveolar partial pressures. All pressures were corrected for water vapour pressure, assuming that the respiratory system was fully saturated at 37 °C. For an animal breathing at the surface, we assumed that alveolar partial pressures of N_2 (PA_{N_2}), O_2 (PA_{O_2}) and CO_2 (PA_{CO_2}) were, respectively, 0.74 ATA, 0.143 ATA (108.9 mmHg, Stephenson, 2005a) and 0.055 ATA (41.9 mmHg Stephenson, 2005a), with 0.062 ATA being water vapour. We assumed that all CO_2 that exchanged for O_2 remained in gas phase.

The fraction of N_2 (F_{N_2}), O_2 (F_{O_2}) and CO_2 (F_{CO_2}) in the lung was computed at each time step after gas had been taken up or transferred to the arterial blood as

$$F_x = n_x \cdot (nN_2 + nO_2 + nCO_2)^{-1} \quad (2)$$

where F_x is the fraction of gas x and n_x (nN_2, nCO_2 and nO_2) are the number of moles of gas x (N_2, CO_2 and O_2, respectively). Alveolar partial pressures were computed as the product between the ambient pressure (P_{amb}) and F_x. Lung volume (V_L) was adjusted with removal or addition of gas to the lung according to the ideal gas law.

2.3. Blood gas stores

The blood was divided up into small packages that held N_2, O_2 and CO_2. The content of N_2 (CV_{N_2}), CO_2 (CV_{CO_2}) and O_2 (CV_{O_2}) in each package (l O_2 at 37 °C l^{-1} blood) was determined by

$$Cv_{N_2} = P_{N_2} \cdot \alpha_{N_2} \quad (2A)$$

for N_2 and by

$$Cv_{CO_2} = [(1 - S) \cdot A_0 \cdot P_{CO_2}^{B_0} + S \cdot A_1 \cdot P_{CO_2}^{B_1}] \quad (2B)$$

for CO_2 and by

$$Cv_{O_2} = S \cdot C_{Hb} \cdot \beta_{Hb} + P_{O_2} \cdot \alpha_{O_2} \quad (2C)$$

for O_2. In these equations, α_{N_2} and α_{O_2} are the Ostwald solubility coefficients for N_2 and O_2, respectively (l gas at 37 °C l^{-1} fluid·ATA-1, Weathersby and Homer, 1980). A_0 and B_0 are parameters relating P_{CO_2} to CV_{CO_2} for deoxygenated blood, and A_1 and B_1 for oxygenated blood. C_{Hb} is the concentration of haemoglobin and β_{Hb} the haemoglobin O_2 binding capacity. S is the O_2 saturation (%) given by

$$S = P_{O_2}^{{}^nHb} \cdot (P_{O_2}^{{}^nHb} + P_{50_{Hb}}^{{}^nHb})^{-1} \quad (3A)$$

where ${}^n_{Hb}$ is the Hill coefficient and $P_{50_{Hb}}$ the PO_2 at 50% saturation. The parameters in Eqs. (2B), (2C) and (3A) were determined from the properties reported for the bladdernose seal (currently called hooded seal, Clausen and Ersland, 1969) and are given in Table 1. P_{CO_2} was directly proportional to P_{50} for seal blood and therefore we estimated the Bohr effect as:

$$P_{50} = 0.02326 + 0.1465 \cdot P_{CO_2} \quad (3B)$$

2.4. Tissue gas stores

Tissue CV_{N_2} was determined by Eq. (2A). The N_2 solubility in the fat and brain compartment were given a tissue-blood partition coefficient of 5 while for all other tissues it was assumed that N_2 solubility was identical to that of blood (Weathersby and Homer,

Table 1
Parameter values used to estimate O_2 and CO_2 content (Eqs. (2A)–(2C) and (3A)–(3B)).

Parameter	Value	Abbreviation
A_0	1.997	
B_0	0.520	
A_1	2.125	
B_1	0.623	
Hemoglobin O_2 binding capacity (l O_2·kg^{-1} Hb)	1.34	β_{Hb}
Hemoglobin concentration (kg Hb·l^{-1} blood)	0.26	C_{Hb}
Hemoglobin Hill coefficient	2.39	n_{Hb}
Hemoglobin $_{P50}$ (ATA)	Eq. (3B)	P_{50Hb}
Myoglobin Hill coefficient	1.01	n_{Mb}
Myoglobin $_{P50}$ (ATA)	0.0016	P_{50Mb}

Table 2
Compartment size, cardiac output ($\dot{Q}_{tot}$ O_2, l O_2 min^{-1}), surface metabolic rate and O_2 stores of a 100 kg phocid seal.

	Compartment size (% of M_b)	$\dot{Q}_{tot}$(l min^{-1})	$\dot{V}_{O_2}$(ml O_2 min^{-1})	O_2 stores (l)
CC	4.53	11.45	162	0.007
M	46.9 (35)	24.75	104	2.512
B	0.13	0.48	4	0.001
F	27.11	0.26	20	0.237
Blood	21.33	–	–	6.360
Total	100	36.94	290	9.117

For muscle, the percentage in parenthesis is the size of the muscle mass used to estimate O_2 stores. O_2 stores excluded lung stores as these depend on the diving lung volume. Compartments are central circulation (CC), muscle (M), brain (B), fat (F) and arterial and venous blood (Blood).

1980). Dissolved tissue CV_{CO_2} and CV_{O_2} were estimated by equations similar to Eq. (2A), using gas tensions for CO_2 and O_2 Ostwald coefficients. The Ostwald solubility coefficients for CO_2 for the central circulation and muscle was 0.631 CO_2·l tissue^{-1}, for the fat compartment 1.361 CO_2·l tissue^{-1}, and for brain 0.561 CO_2·l tissue^{-1} (Weathersby and Homer, 1980). The O_2 solubility for the central circulation and muscle was 0.02611 O_2·l tissue^{-1} and for the fat and brain compartment a value of 0.1331 O_2·l tissue^{-1} was used (Weathersby and Homer, 1980).

We assumed that only the muscle contained myoglobin bound O_2. The O_2 content of the muscle was estimated using Eq. (2C) with parameters for n_{Mb} and P_{50Mb} specific for myoglobin for a deep diving animal (Table 1, Tamburrini et al., 1999). It was assumed that the P_{50Mb} is not affected by changes in P_{CO_2} (Gayeski et al., 1987).

2.5. Gas exchange

2.5.1. Tissue and lung

The blood packages were transferred around the circulatory system at a rate determined by cardiac output ($\dot{Q}_{tot}$, l min^{-1}). Each tissue received a portion of the blood in each package representing its fraction of total blood flow. To account for the specific metabolic rate of each tissue, a given volume of O_2 was removed from the blood while CO_2 was added to the tissue. Next, the tissue was allowed to exchange gas with the blood and it was assumed that the exchange between blood and tissue was complete once the blood left the capillary. In other words, the partial pressure of each gas was equal in blood and tissue as the blood left the capillary. At the surface, a similar equality was assumed at the lung-blood interface. That is, pulmonary end-capillary blood tension for each gas was assumed equal to the alveolar partial pressure. During diving, on the other hand, a pulmonary shunt developed as a consequence of the compression of the respiratory system (see below).

2.6. Lung compression and pulmonary shunt

The model recently published by Bostrom et al. (2008) was used to estimate alveolar volume (DV_A) at depth. Total lung capacity (TLC) included the volume of the dead space (trachea and bronchi, V_D), and the maximum alveolar volume (V_A), i.e. TLC = V_D + V_A. It was assumed that gas exchange only occurred in the alveoli and when DV_A = 0, gas exchange stopped. For the elephant seal, TLC was assumed to be 50 ml kg^{-1} and for the Weddell seal 40 ml kg^{-1} (Kooyman et al., 1972; Kooyman and Sinnett, 1982). Dead space volume was 10% of TLC (Stephenson, 2005a). Diving lung volumes were taken from previous studies (Kooyman et al., 1972; Kooyman and Sinnett, 1982) and were 20.4 ml kg^{-1} for the elephant seal (Kooyman et al., 1972), 22.0 ml kg^{-1} for the Weddell seal (Kooyman et al., 1972; Kooyman and Sinnett, 1982). As DV_L was lower than TLC, i.e. pre-dive exhalation or partial inhalation, the reduced gas volume was subtracted from the alveolar gas space. That is, DV_A before a dive (DV_{Ao}) was $DV_{Ao} = DV_L - V_D$. Thus, for a 100 kg elephant seal V_D = 0.5 l, DV_L = 2.04 l, DV_{Ao} = 1.54 l.

To determine the relationship between pulmonary shunt and compression collapse a prediction equation was created from previously published pulmonary shunt data and the estimated ratio $DV_A \cdot V_A^{-1}$. The multivariate linear regression published for harbour seals diving in a hyperbaric chamber, relating pulmonary shunt to ambient pressure (P_{amb}) and DV_L (shunt = 34.8 + 5.1 P_{amb} − 0.43 l, Kooyman and Sinnett, 1982), was used to obtain estimates of the shunt at a number of different pressures (3–11 ATA) and DV_L's (100–20% of TLC). The corresponding DV_L's were used to estimate $DV_A \cdot V_A^{-1}$ at pressures in the same range. Finally, the relationship between shunt and $DV_A \cdot V_A^{-1}$ was determined using a power function (Bostrom et al., 2008) for data from both harbour seals and California sea lions.

$$\text{Shunt} = 1 - (a \cdot (DV_A \cdot V_A^{-1})^{-b}) \quad (4)$$

2.7. Compartment size, cardiac output and blood flow distribution

In the absence of direct anatomical or physiological data for the elephant seal, data reported for the Weddell seal were used (Davis and Kanatous, 1999). We assume no differences between the elephant seal and the Weddell seal except for M_b. The relative size of each compartment was 46.90% for the muscle compartment (with 35% as muscle mass), 4.53% for central circulation, 0.13% for brain, 21.33% for blood and 27.11% for fat (Table 2). The muscle compartment included muscle and all other tissues that were not included in central circulation, fat and brain, e.g. skin, bone, connective tissue. As myoglobin is only present in the muscle, the percent of M_b used to calculate the O_2 store was 35%, i.e. muscle only (Table 2).

In this model, $\dot{Q}_{tot}$ at the surface was assumed to be in the midrange (8.0 ml kg^{-1} s^{-1}, range 3–12 ml kg^{-1} s^{-1}) of those measured for harbour seals (M_b range 28–39 kg) swimming at different work loads (Ponganis et al., 1990). To account for differences in M_b, mass specific $\dot{Q}_{tot}$($s\dot{Q}_{tot}$) was adjusted using the equation presented by Davis and Kanatous (1999) for allometrically adjusting $\dot{V}_{O_2}$. Thus, $s\dot{Q}_{tot}$ was estimated by:

$$s\dot{Q}_{tot} = 8 \cdot (M_b^{-0.25} \cdot 34^{-0.25}) \quad (5)$$

where 8 and 34 are, respectively, the $\dot{Q}_{tot}$ and M_b of the harbour seals (Ponganis et al., 1990). We assumed that the reduction in $\dot{Q}_{tot}$ associated with submergence was between 1/2 and 1/3 of the surface value, quantitatively similar to the reduction in heart rate measured in freely diving elephant seals (Andrews et al., 1997). Blood flow distribution to each tissue at the surface was assumed similar to that measured in Weddell seals resting at the surface (Zapol et

Table 3
Effect of different lung collapse models on estimated PN_2 values for two dives (to 70 m and to 305 m) based on parameters for a 100 kg elephant seal.

Depth (m)		Lung collapse model	End dive PN_2 (ATA)					Max dive P_{N_2} (ATA)				
(m)	Model		CC	M	B	F	V	CC	M	B	F	V
70	A	GC_{HS}	3.08	0.87	3.09	0.97	1.58	3.79	1.00	3.78	0.97	3.55
70	B	I_{30}	0.86	0.75	0.86	0.76	0.79	1.43	0.82	1.37	0.76	1.35
70	C	I_{70}	2.96	0.81	2.84	0.83	1.49	3.51	0.91	3.35	0.83	3.22
70	E	N	2.89	0.87	2.94	1.00	1.53	4.68	0.92	4.59	1.00	4.36
70	F	$GC_{HS\text{-}O2\&CO2}$	3.00	0.86	3.02	0.97	1.55	3.67	0.96	3.67	0.97	3.44
305	A	GC_{HS}	2.55	0.87	2.58	0.98	1.41	3.52	0.98	3.50	0.98	3.30
305	B	I_{30}	0.82	0.75	0.82	0.76	0.77	1.43	0.82	1.37	0.76	1.35
305	C	I_{70}	2.84	0.82	2.70	0.86	1.46	3.51	0.93	3.35	0.86	3.22
305	D	I_{160}	1.92	0.94	1.96	1.15	1.25	6.16	0.96	6.04	1.15	5.72
305	E	N	1.85	0.95	1.88	1.18	1.24	6.16	0.96	6.04	1.18	5.72
305	F	$GC_{HS\text{-}O2\&CO2}$	2.64	0.90	2.66	1.05	1.46	4.44	0.98	4.41	1.05	4.14

N = no collapse, GC = graded compression with pulmonary shunt estimated from data for harbour seal (GC_{HS}, Bostrom et al., 2008), I = instantaneous collapse at 30 m (I_{30}), 70 m (I_{70}), or 160 m (I_{160}). Maximum and end dive P_{N_2} in central circulation (CC), muscle (M), brain (B), fat (F) and mixed venous (V) blood is presented. Initial diving lung volume was 20.4 ml kg^{-1}. Model F includes the pulmonary shunt model (Bostrom et al., 2008) but excludes exchange of O_2 and CO_2 (Fahlman et al., 2006, 2007).

al., 1979), where 31% of $\dot{Q}_{tot}$ was directed to the central circulation, 67% to the muscle (psoas, diaphragm, intercostal, testis, pituitary, thyroid, pancreas, adrenals, rib/bone, skin, spleen, retina, tongue, vagina, uterus, ovary), 1.3% to the brain and 0.7% to the fat (Zapol et al., 1989). During diving, on the other hand, the blood flow distributions were iteratively tested to maximize utilization of O_2 to increase the aerobic dive duration.

2.8. Model variations

Two hypothetical dives were created for a 100 kg elephant seal. The dives were chosen to resemble the average dive on and off the continental shelf for an elephant seal (Andrews et al., 1997) and consisted of a single dive to 70 m for 10 min or a 17 min dive to 305 m. Each dive had a constant and symmetrical descent and ascent rate of 2.0 m s^{-1}. $\dot{Q}_{tot}$ at the surface was 36.9 and 18.5 l min^{-1} while diving. Blood flow distribution was as detailed above while at the surface and during diving 80% of $\dot{Q}_{tot}$ was directed to the central circulation, 1% to the muscle, 12% to the brain and 7% to the fat. These variables are considered the standard model (Model A, Table 3), and this was compared with those assuming a linearly increasing diffusion rate with depth followed by an immediate decrease to 0 at the collapse depth.

2.9. The effect of changes in DV_L on N_2 uptake during a single dive

To investigate how pre-dive exhalation, or partial inhalation, affected gas exchange during diving Model A was repeated as detailed above for dives to 70 and 305 m with DV_L varied between 20% and 100%, while pre-dive V_D was kept constant at 0.5 l.

2.10. Comparing the model output with measured data

The model was used to estimate blood and tissue P_{O_2}, P_{CO_2} and P_{N_2} and we compared estimated values to data from previous studies that either directly measured blood and tissue P_{O_2}, P_{N_2} and P_{CO_2} (Kooyman et al., 1972; Kooyman et al., 1973; Qvist et al., 1986), or from respirometry data (Kooyman et al., 1973; Ponganis et al., 1993).

2.10.1. Weddell seal PA_{O_2} measurements

We compared our model estimates for PA_{O_2} for a 450 kg adult Weddell seal, with observed data on PA_{O_2} collected for several dives (Table 4 in Ponganis et al., 1993). As the metabolic rate changed with dive duration we adjusted the mass specific rate of O_2 consumption ($s\dot{V}_{O_2}$) accordingly. At the surface and for dives <10 min $s\dot{V}_{O_2}$ was 5.0 ml O_2 kg^{-1} min^{-1}, for a dive ≥ 10 min and <20 min $s\dot{V}_{O_2}$ was 2.5 ml O_2 kg^{-1} min^{-1} and for dives ≥20 min $s\dot{V}_{O_2}$ was set at 1.7 ml O_2 kg^{-1} min^{-1}. There was one dive that was exceptionally long (dive # 9, 57 min) but this was not used in this analysis as the observed respirometry data was not reliable. The myoglobin concentration was measured to be 4.2 g × 100 g $muscle^{-1}$ for this seal (Ponganis et al., 1993). We assumed $\dot{Q}_{tot} = 42.7$ l min^{-1} at the surface with a 50% reduction during diving. The blood flow distribution while diving was 60% to central circulation, 35% to the muscle, 3% to the brain and 2% to the fat compartment. Due to a lack of information we assumed all dives had a constant descent and ascent rate of 1.5 m s^{-1} (Andrews et al., 1997). Dives ≤2 min were assumed to be to 20 m, dives ≤ 10 min to 40 m and all other dives to 160 m (Burns, 1999).

2.10.2. Elephant seal P_{N_2} measurements

Estimates of Pa_{N_2} and venous Pv_{N_2} were compared with observed values during forced dives in elephant seals (Kooyman et al., 1972). We limited the model calibration of N_2 levels to this one study and species as we were able to obtain heart rates (f_H, Kooyman pers. comm.), DV_L and time specific values for blood P_{N_2} for this species (Kooyman et al., 1972). Mixed venous P'_{N_2}s (Pv_{N_2}) and Pa_{N_2}s reported for forced diving (4–28 ATA) were compared with the output from Model A for an animal weighing 104 kg. As the animal was not active during these forced dives, we used a conservative estimate for $\dot{Q}_{tot}$ (19.4 l min^{-1}) at the surface. The average heart rate was ~115 beats min^{-1} at the surface and 15 beats min^{-1} during a dive to 4 ATA, 11 beats min^{-1} for a dive to 7.8 ATA and 22 beats min^{-1} for a dive to 14.6 ATA (Kooyman pers. comm). From these data, we assumed that $\dot{Q}_{tot}$ during diving was 12.5% of the surface value. Blood flow distributions used during diving were CC: 45%, M: 40%, B: 14%, F: 1%. To test the effect of ascent exhalation on gas exchange, the model was run for the deep dive with a shunt of 80% during the ascent as well as while the animal was still submerged at the surface (1 ATA).

3. Results

3.1. Pulmonary shunt and gas exchange

The relationship between estimated shunt and $DV_A \cdot V_A^{-1}$ available for the harbour seal (Kooyman and Sinnett, 1982) was fitted with a power function ($P < 0.001$, $r^2 = 0.96$, Fig. 1) resulting in the following equation

$$\text{Shunt}_{HS} = 1 - 1.495 \cdot (DV_A \cdot V_A^{-1})^{0.320} \quad (6A)$$

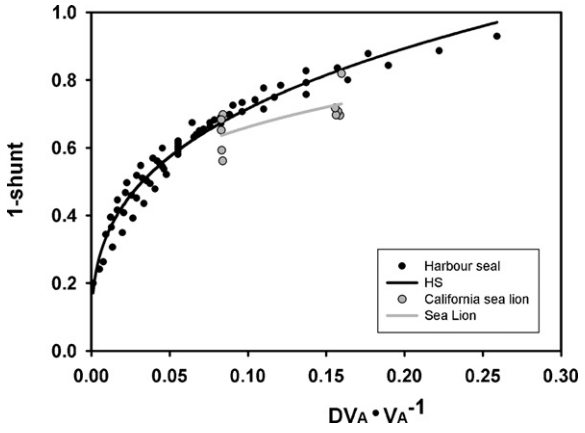

Fig. 1. Estimated fractional alveolar volume ($DV_A \cdot V_A^{-1}$) against observed pulmonary shunt (1-shunt) in harbour seals (black filled circles) and California sea lions (red filled circles). The data was fitted with a power function (Eq. (4)) and the resulting best fit is shown as a solid line.

This equation results in a 100% shunt when the alveoli collapse. As no information exists on gas exchange at very low lung volumes, collapse was assumed to occur when $DV_A \cdot V_A^{-1} \leq 0.001$. The maximum shunt before collapse was therefore 83.6%. For $DV_A \cdot V_A^{-1}$ >28.5% V_A the shunt was negative and therefore set to 0. The estimated data for the California sea lion fell on or slightly below the best fit line for harbour seals (Fig. 1). The best fit power function was ($P < 0.05$, $r^2 = 0.46$, Fig. 1)

$$\text{Shunt}_{CSL} = 1 - 1.072 \cdot (DV_A \cdot V_A^{-1})^{0.210} \quad (6B)$$

3.2. The effect of changes in DV_L on N_2 uptake during a single dive

Fig. 2 shows the effect of a constant V_D (0.5 l) and a variable DV_L (50 ml kg^{-1}, 40 ml kg^{-1} ml kg^{-1}, 30 ml kg^{-1}, 20 ml kg^{-1} and 10 ml kg^{-1}) on Pa_{N_2} and Pv_{N_2} for a 100 kg elephant seal during a dive to 70 m (Fig. 2A and B) and 305 m (Fig. 2C and D). It was assumed that the animal experienced a 50% reduction in blood flow (due to vasoconstriction) during the dive and the blood flow distributions were the same as in Model A. For a dive to 70 m, maximum Pa_{N_2} decreased by 56% and Pv_{N_2} decreased 63% as the ratio between V_D and DV_{Ao} ($DV_{Ao} \cdot V_D^{-1}$) decreased from 9 to 1

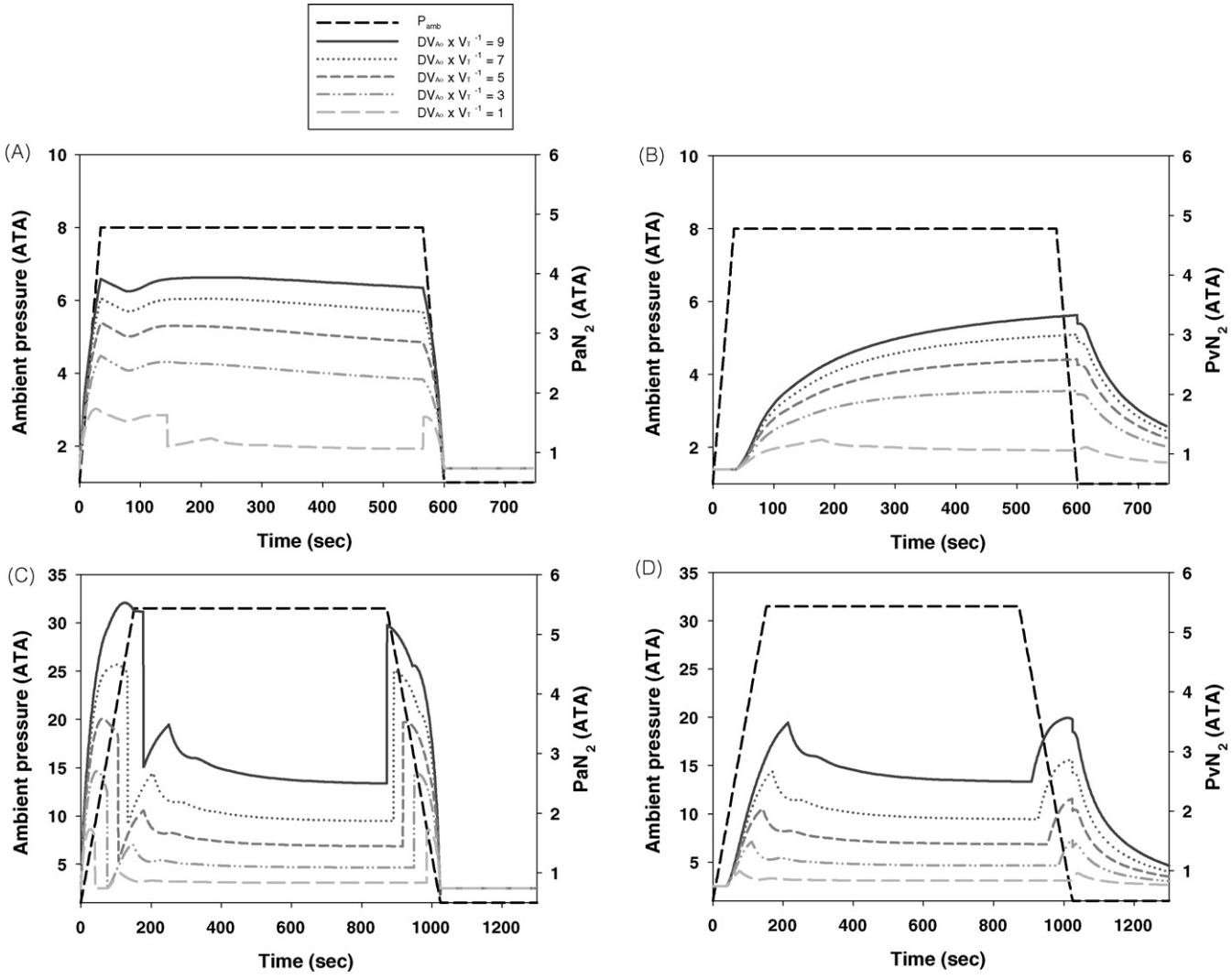

Fig. 2. Estimated arterial (Pa_{N_2}, panel A and C) and mixed venous N_2 (Pv_{N_2}, panel B and D) tensions (ATA) for a dive to 70 m (panel A and B) or 305 m (panel C and D), assuming a constant dead space volume of 0.5 l (V_D) for a 100 kg elephant seal. DV_L was varied between 50 and 10 ml kg^{-1} and initial alveolar volume (DV_{Ao}, l) estimated as: $DV_{Ao} = DV_L - V_D$.

(Fig. 2A). For a $DV_{Ao}{\cdot}V_D^{-1}$ ratio of 1, the alveoli collapsed 145 s into the dive (Fig. 2A). Pa_{N_2} before alveolar collapse was 1.63 ATA and dropped immediately to 1.11 ATA, the corresponding Pv_{N_2} 37 s earlier, i.e. 108 s into the dive. During a dive to 305 m, alveolar collapse occurred for all $DV_{Ao}{\cdot}V_D^{-1}$ ratios (Fig. 2C and D). Only for a $DV_{Ao}{\cdot}V_D^{-1}$ ratio of 9 were the alveoli open during the entire descent, but they collapsed soon after the bottom had been reached as removal of N_2 from the lung decreased the lung volume. Maximum Pa_{N_2} decreased by 69% as $DV_{Ao}{\cdot}V_D^{-1}$ decreased from 9 to 1 (Fig. 2C). Collapse depth increased exponentially as $DV_{Ao}{\cdot}V_D^{-1}$ increased ($r^2 = 0.99$, $P < 0.01$) according to

$$\text{Collapse depth} = 274.5 \cdot (1 - e^{(-0.309 \cdot [DV_{Ao} \cdot V_D^{-1}])}) \quad (7)$$

As the alveoli collapsed, Pa_{N_2} decreased to a value equivalent to Pv_{N_2} 37 s earlier. For a $DV_{Ao}{\cdot}V_D^{-1}$ ratio ≤ 3, this meant that Pa_{N_2} decreased to ambient P_{N_2} (0.74 ATA). Following the alveolar collapse, Pa_{N_2} traced Pv_{N_2} until the alveoli were again recruited during ascent.

End dive Pv_{N_2} increased exponentially as $DV_{Ao}{\cdot}V_D^{-1}$ increased for dives to 70 m and the relationship was

$$\text{End dive } P_{N_2} = 3.26 \cdot (1 - e^{(-0.312 \cdot [DV_{Ao} \cdot V_D^{-1}])}) \quad (8A)$$

showing that the end dive P_{N_2} decreased relatively more for a given decrease in the $DV_{Ao}{\cdot}V_D^{-1}$ ratio. For the dive to 305 m, on the other hand, Pv_{N_2} increased linearly as $DV_{Ao}{\cdot}V_D^{-1}$ increased

$$\text{End dive } Pv_{N_2} = 0.362 + 0.3315 \cdot [DV_{Ao} \cdot V_D^{-1}] \quad (8B)$$

It can therefore be seen that there is no simple relationship between these variables and pressure.

3.3. Estimated metabolic gas tensions

Fig. 3 shows pulmonary shunt, Pa_{O_2}, Pa_{CO_2}, mixed venous P_{O_2} (Pv_{O_2}) and P_{CO_2} (Pv_{CO_2}) for a single dive to 70 m in a 100 kg elephant seal presented in Table 3 (Model A). DV_L was 20.4 ml kg^{-1}, $\dot{Q}_{tot}$ at the surface was set at 36.9 l min^{-1} with a 50% reduction during diving.

Pa_{CO_2} increased rapidly during the descent phase, causing a spike in Pa_{CO_2} with a maximum at 6 m (0.066 ATA) followed by a rapid decline to 0.058 ATA, a value 5% higher than the pre-dive Pa_{CO_2} (Fig. 3A). Pv_{CO_2} increased immediately upon submergence as the blood flow distribution changed, and a sharp peak appeared during descent with a maximum of 0.067 ATA occurring at 5.5 ATA (45 m), 0.45 min into the dive (Fig. 3B). Following the descent peak, both Pa_{CO_2} and Pv_{CO_2} cycled with a period equal to the blood transit time during diving (66 s, 22 s arterial and 44 s venous) although each cycle was out of phase by 22 s. Both PA_{CO_2} and Pv_{CO_2} showed an overall increase throughout the dive with Pa_{CO_2} reaching 0.077 ATA (58.5 mmHg) immediately before decompression and Pv_{CO_2} reaching 0.084 ATA upon return to the surface (Fig. 3).

Lung compression during descent increased Pa_{O_2} to a maximum of 0.226 ATA (172 mmHg) at 3 ATA, an increase of 59% from Pa_{O_2} at the surface (Fig. 3A). After the maximum, Pa_{O_2} declined exponentially to a minimum of 0.045 ATA immediately before surfacing. Pv_{O_2}, on the other hand, showed an abrupt drop from 0.112

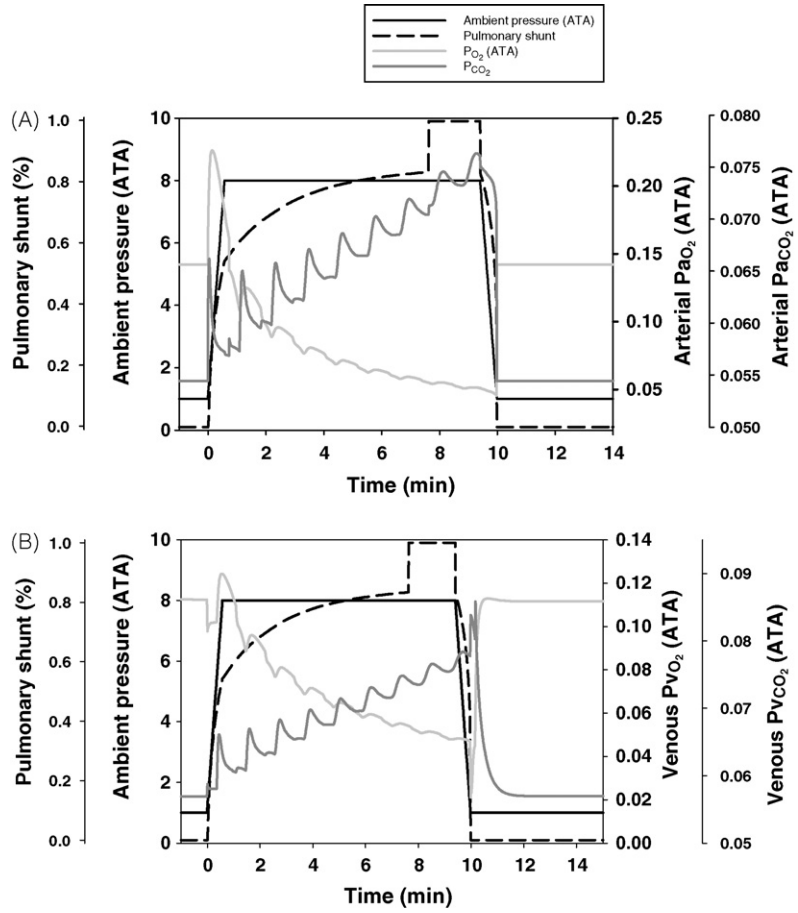

Fig. 3. Estimated A) arterial (Pa_{O_2}, Pa_{CO_2}) and B) venous (Pv_{O_2}, Pv_{CO_2}) O_2 and CO_2 tensions (ATA) during a dive to 70 m for 10 min for a 100 kg elephant seal. $\dot{Q}_{tot}$ during diving was 50% of the surface value and 80% of the blood flow was directed to the central circulation, 1% to the muscle, 12% to the brain and 7% to the fat. The diving lung volume at the start of the dive was 20.4 ml kg^{-1} with a dead space volume of 0.5 l.

ATA to 0.098 ATA as the blood flow distribution changed upon immersion (Fig. 3B). This was followed by an increase that lagged behind the arterial peak and that reached 0.124 ATA. As the animal approached the surface, Pa_{O_2} decreased more rapidly and at 20 m the rate of decline had doubled compared to that at 70 m. This more rapid decline was caused by the expanding respiratory system and, together with changes in the blood flow distribution upon surfacing, resulted in a large drop in Pv_{O_2} soon after surfacing.

The pulmonary shunt increased during the descent, reaching 54% at the maximum depth, 8 ATA. The shunt continued to increase asymptotically throughout the dive as gas was absorbed by the body. Lung collapse, i.e. 100% pulmonary shunt, finally occurred 7.6 min into the dive.

3.4. Comparing the model output with measured data

3.4.1. Weddell seal PA_{O_2} measurements

Fig. 4 shows observed and estimated end dive PA_{O_2} from a 450 kg adult Weddell seal. Open circles show data from short dives (≤5 min) while the solid circles are from long dives (>5 min). The model underestimated ([predicted − observed]·observed^{-1}·100) observed values by −1% (range: 73% to −47%). When separated into short and long dives, the error was −9% (range 17% to −39%) and 5% (range 73% to −47%), respectively. Estimated end dive PA_{O_2} for the 57 min dive was 10 mmHg. Pa_{O_2} for the longest dive is not shown as the observed data was not reliable.

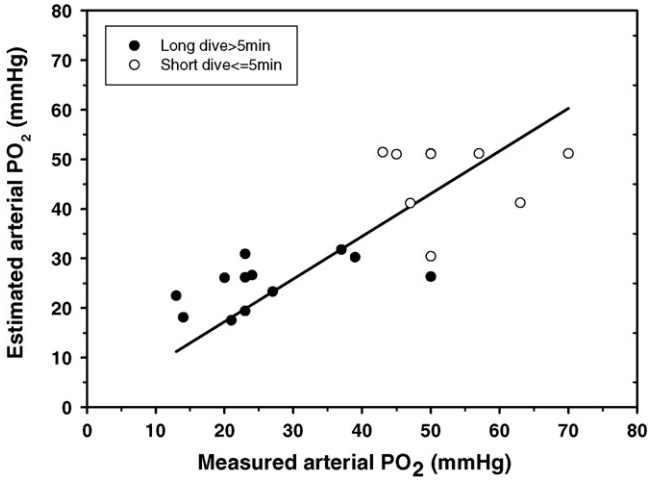

Fig. 4. Estimated vs. observed end-tidal (alveolar) P_{O_2} (PA_{O_2}) for a 450 kg Weddell seal. Observed data were reported in Ponganis et al. (Table 4, 1993). Open circles are for short dives (<5 min) and closed circles are for long dives (≥5 min).

When the model was run without a reduction in $\dot{Q}_{tot}$ during diving, the PA_{O_2} for long dives were overestimated by 11% and the short dives underestimated by −6%. With $\dot{Q}_{tot}$ at 25% of the surface value during diving, the predicted values for the long and short dives were −10% and 28%, respectively. With a diving $\dot{Q}_{tot}$ that was

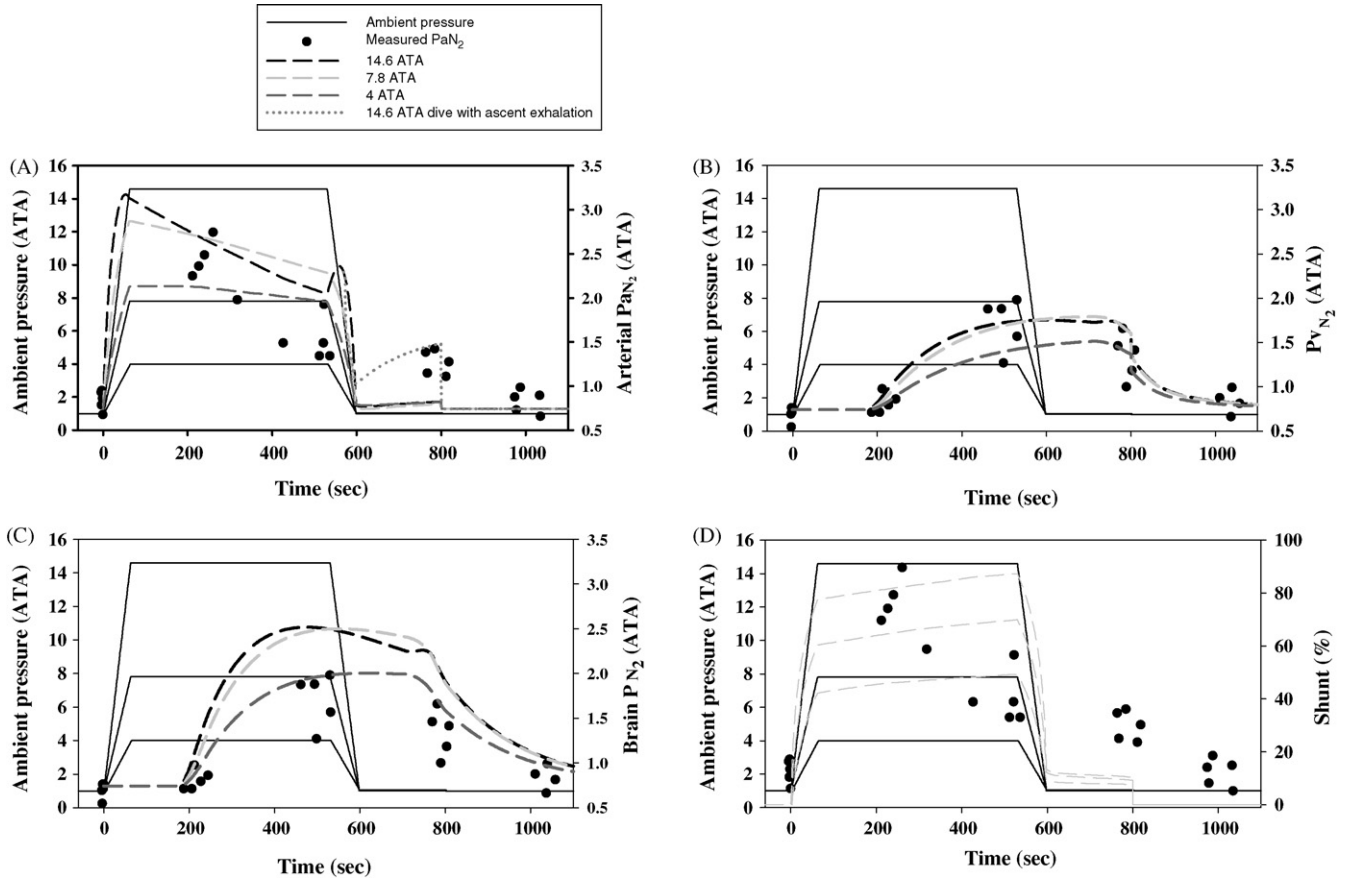

Fig. 5. Observed arterial and intravertebral P_{N_2} (Kooyman 1972) vs. estimated A) arterial (Pa_{N_2}), B) mixed venous (Pv_{N_2}) and C) brain P_{N_2} for a 104 kg elephant seal to 4, 7.8 or 14.6 ATA for durations similar to those reported by Kooyman et al. (1972). Filled circles are observed data, solid black line shows the ambient pressure, dashed lines show estimated P_{N_2} for a dive to 14.6 ATA (black), 7.8 ATA (light gray), and 4 ATA (dark gray). The dotted gray line in panel A shows Pa_{N_2} for a dive to 14.6 ATA in which the seal exhaled during the dive thereby maintaining a constant pulmonary shunt. In panel D, dashed gray lines show the pulmonary shunt for each of the dives as shunt increases with pressure.

50% of the surface value, an increase in DV_L (50 ml kg^{-1}) resulted in an overestimation of Pa_{O_2} by 11% with a range from 81% to −51%. With a DV_L of 10 ml kg^{-1}, the error decreased to 2% with a range from 74% to −45%.

3.4.2. Elephant seal P_{N_2} measurements

We initially used a blood flow distribution during diving that was similar to those measured in force-dived Weddell seals (CC: 34%, M: 51%, Br: 14.5%, F: 0.5%, Kooyman et al., 1972). However, this depleted O_2 before the end of the dive for the central circulation and the fat. We therefore adjusted the blood flow distribution so that more blood was going to the central circulation (45%) and fat (1%) while less was directed to the muscle (40%) and the brain (14%).

Measured Pa_{N_2} during dives to depths between 30 and 136 m (4 ATA to 14.6 ATA) ranged from 1.34 ATA to 2.74 ATA and did not differ significantly with depth (Kooyman et al., 1972). Until 400 s into the dive, there was reasonable agreement between estimated and observed Pa_{N_2} (Fig. 5). After 400 s into the dive, Pa_{N_2} from the model mostly overestimated observed values by between 0.5 ATA and 0.9 ATA (Fig. 5). Estimated pulmonary shunt when reaching 4 ATA was 42%, at 7.8 ATA it was 60% and at 14.6 ATA 77%. The pulmonary shunt increased during the time at depth, as O_2 and N_2 were taken up, reaching a maximum of 49% at 4 ATA, 70% at 7.8 ATA and 87% at 14.6 ATA.

In the study by Kooyman et al. (1972) the seals were kept submerged after having returned to the surface so blood samples could be taken while still holding their breath. The average observed (±1 SD, all $n = 5$) Pa_{N_2} (1.27 ± 0.14 ATA) at this time was significantly higher than those before the dive (0.84 ± 0.11 ATA) and 200 s after the seal had begun breathing (0.83 ± 0.13 ATA, $P < 0.01$ 1 way ANOVA with Bonferroni correction post-hoc analysis). Average predicted Pa_{N_2} at 1 ATA while still submerged, on the other hand, was 0.78 ATA and 200 s after the end of the submersion it was 0.75 ATA (Fig. 5). While still submerged at 1 ATA, predicted pulmonary shunt was 9% after the dive to 4 ATA and 14% after the dive to 14.6 ATA. The predicted shunt decreased slightly as N_2 exchanged with the pulmonary capillary and entered the lung, but was still >7% at the end of the submersion (at 800 s) immediately before the animal could breathe. When the predicted pulmonary shunt was maintained at 80% throughout the ascent after the dive to 14.6 ATA, i.e. caused by exhalation during the dive, estimated Pa_{N_2} upon reaching 1 ATA was 1.02 ATA and increased to 1.48 ATA at the end of the submersion.

Measured P_{N_2} from the intravertebral vein, in which cerebral flow is a major component, was similar to or slightly higher (average 0.81 ATA, 0.71 to 0.98 ATA) than estimated Pa_{N_2} and Pv_{N_2} (0.70 ATA) before the dive (Fig. 5B and C). Immediately before decompression, intravertebral P_{N_2} had increased to between 1.27 ATA and 1.98 ATA (average 1.72 ± 0.29 ATA). After 200 s at 1 ATA while still submerged, average intravertebral P_{N_2} had decreased to 1.34 ± 0.26 ATA (range: 1.00–1.66 ATA) and 200 s after the end of the dive it had further decreased to 0.84 ± 0.14 ATA. The Pv_{N_2} estimates agreed fairly well with observed intravertebral P_{N_2} during and after the dive, but all estimates underestimated the maximum values observed before decompression (Fig. 5B). Estimated brain P_{N_2}, on the other hand, generally overestimated observed values (Fig. 5C)

3.5. Comparing end dive P_{N_2} estimates with previous models

An analysis that tested the effect of adjusting variables that determined the degree of pulmonary shunt with depth is presented in Table 3. Model A is the base model to which all other models are compared. Model F, which is the same as Model A but does not account for exchange of O_2 and CO_2, can be seen to have relatively little effect on P_{N_2} values compared to the other models. For the dive to 70 m, not accounting for exchange of O_2 and CO_2 (Model F) decreased end dive P_{N_2} by 0.6–2.8% compared with Model A. For the dive to 305 m, on the other hand, end dive P_{N_2} increased by 3.3–7.2% when not accounting for the metabolic gases.

Compression between models with differing lung collapse assumptions showed much greater variability (Table 3). For a dive to 70 m, the lung collapsed after 7.6 min into the dive for Model A leading to end dive Pv_{N_2} approximately twice the surface value (Table 3). For the dive to 305 m, gas exchange ceased at 176 m for Model A and end dive P_{N_2} was lower than the shorter and shallower dive to 70 m using the same model (Model A 70 m vs. 305 m). When the pulmonary shunt was assumed to occur instantaneously at 30 m, Pv_{N_2} decreased by 50% for a 70 m and 45% for a 305 m dive compared with Model A (Model A vs. B). The reduction in end dive P_{N_2} of the other tissues was between 14% and 72% for the dive to 70 m and between 14% and 68% for the dive to 305 m (Table 3, Model A vs. B). With a collapse depth of 70 m (Model C), or without lung collapse (Model E), end dive P_{N_2} was similar to Model A for the 70 m dive. For the 305 m dive, collapse at 70 m increased end dive P_{N_2} in the fast tissues (CC and B) while it decreased in F and M (Table 3 Model A vs. C) while for the model with without collapse (Model E), end dive P_{N_2} decreased compared with Model A. End dive P_{N_2} was greater for a 70 m lung collapse depth (Model C) than it was for a 30 m lung collapse depth (Model B) for both dive depths. However, counter intuitively, with a lung collapse depth of 160 m (Model D) or without lung collapse (Model E), end dive P_{N_2} decreased for CC B and mixed venous (Model C vs. D, or Model C vs. E) for the dive to 305 m.

4. Discussion

In this paper, we present a model to estimate how gas exchange is altered during breath-hold diving. This is the first comprehensive attempt to quantify how gas exchange is affected by the physical parameters and variables of a marine mammal's respiratory system. The current model differs from previous models in two significant ways. First, it includes an estimation of the volumes of the respiratory system allowing a more realistic prediction of pulmonary shunt. Secondly, it includes uptake and removal of O_2 and CO_2. Our model provides interesting and, at times, counter-intuitive predictions that emphasize the importance of this type of modelling approach to understand the complex physiological events that underlie how diving mammals manage metabolic and inert gases.

Despite the fact that Scholander proposed that the alveoli collapse in marine mammals during diving well over half a century ago, few studies have verified this hypothesis, partly because of logistical difficulties in measuring lung volumes or gas exchange during diving. Even though much work has and is being conducted to understand how O_2 is managed during diving (Stockard et al., 2007) our understanding of how gas exchange is affected during breath-hold diving is rudimentary at best. Since continued gas exchange during diving may significantly affect blood and tissue O_2, CO_2 and N_2 levels and as studies on large mammals are logistically and ethically challenging, mathematical models are useful to help generate hypotheses as to the mechanics of gas exchange during diving.

4.1. Comparison of the model to measured data

Mathematical models are only as good as the data from which they are constructed. Ground-truthing such models against measured data is therefore vital to establish their validity. We compared model output with both Pa_{O_2} and P_{N_2} data from two previous studies.

Predicted end dive Pa_{O_2} was similar to the observed data for a 450 kg Weddell seal (Fig. 4), despite assumptions of constant $\dot{Q}_{tot}$, blood flow distribution and diving metabolic rate throughout a dive. There were some notable exceptions, however. Predicted end dive Pa_{O_2} was generally around 51 mmHg for short dives. Average predicted Pa_{O_2} underestimated observed values by 9%. The lowest predicted Pa_{O_2} was 30 mmHg and this was the end dive value after the first dive. The first value depends on the previous dive history and this may explain why this value was significantly below the observed Pa_{O_2} of 50 mmHg. For the short dives, the differences could be attributed to an incorrect choice of $\dot{Q}_{tot}$ during diving. Observed Pa_{O_2} for 1 min dives ranged between 45 and 70 mmHg while the model predicted Pa_{O_2} mostly around 51 mmHg. It is possible that the seal did not experience a reduction in $\dot{Q}_{tot}$ during these short underwater excursions and when $\dot{Q}_{tot}$ was kept constant during the dive the difference was reduced. For the long duration dives, predicted values were generally to within 2–3 mmHg (~10–20%) of observed values and the largest error was 9 mmHg. For both long and short dives, the error changed with changes in $\dot{Q}_{tot}$ and DV_L. Improving our understanding how diving animals adjust blood flow and its distribution during diving as well as the effect of pressure on gas exchange will therefore be important to improve our understanding of gas management during diving.

Model P_{N_2} estimates also agreed well with observed data. Kooyman et al. (1972) reported that measured Pa_{N_2} and intravertebral venous P_{N_2} in forced diving elephant seals, diving on 40% of TLC, did not differ with depths ranging between 4 ATA and 14.6 ATA. The model estimated Pa_{N_2} values agreed fairly well up to ~300 s into the dive after which observed Pa_{N_2} was substantially lower (Fig. 5). When the alveoli collapse, Pa_{N_2} should equal Pv_{N_2} and therefore reflect overall N_2 saturation. Observed intravertebral P_{N_2} was similar or higher than Pa_{N_2} before the end of the dive (Kooyman et al., 1972). Such an observation can be explained if the pulmonary shunt was ~100% at the end of the dive or if most of the N_2 in the lung had been taken up by the blood. If the gas exchange rate was higher than predicted by the model or if the seals exhaled during the dive alveolar collapse would occur early in the dive. This may explain the discrepancy in observed and predicted Pa_{N_2}. Predicted Pv_{N_2} agreed fairly well with observed intravertebral P_{N_2} (Fig. 5B). However, a significant portion of the intravertebral vein receives blood from the brain and is therefore not a good estimate of mixed venous blood. This may explain why estimated brain P_{N_2} was slightly higher than observed intravertebral P_{N_2} (Fig. 5C). In other words, P_{N_2} in the intravertebral vein is a mixture of mixed venous (Fig. 5B) and brain (Fig. 5C) blood. Thus, overall the model gives reasonable predictions of blood and tissue P_{N_2} given accurate estimates for pulmonary shunt, $\dot{Q}_{tot}$ and blood flow distribution.

4.2. Addition of O_2 and CO_2 to the model

To investigate the effect of metabolic gases could have on model output, exchange of O_2 and CO_2 was added to the previously published model that only accounted for exchange of N_2 (Fahlman et al., 2006). As gas exchange alters the volume of the lung and also the fractional amount of each gas, it was important to evaluate if addition of the metabolic gases would significantly alter estimated P_{N_2} levels. For the shallow dive that was 10 min in duration, addition of the metabolic gases increased end dive P_{N_2} for all tissues while it decreased P_{N_2} during the deeper and longer dive (Table 3, Model A vs. F). In Model F, PA_{N_2} continually decrease as N_2 is taken up as the pressure increases while it is assumed that O_2 and CO_2 content remain constant. Therefore, less N_2 is taken up during a short dive in Model F compared with Model A (Table 3). With addition of metabolic gases (Model A), O_2 and N_2 is taken up while CO_2 is returned to the lung. The resulting changes in alveolar partial pressures are therefore complex and depend on the metabolic rate, the duration of the dive and the dive depth. In the deep and long dive, therefore, accounting for the metabolic gases (Model A) resulted in end dive tissue tensions that were lower than those for Model F. This shows that despite the rather negligible change in estimated end dive P_{N_2} with the addition of O_2 and CO_2 (Model A vs. F, Table 3), accounting for all pulmonary gases is important to reduce errors. Consequently, previous models that have separately estimated O_2 and CO_2 (Stephenson, 2005a) or N_2 (Fahlman et al., 2006, 2007; Zimmer and Tyack, 2007) will have some extent of error and future studies should assess this.

Estimated data for the metabolic gases during the 10 min dive to 70 m shows how the hydrostatic compression of the respiratory system increases the pulmonary partial pressures during descent (Fig. 3), resulting in a spike in Pa_{O_2} and Pa_{CO_2}. Estimated maximum Pa_{O_2} (172 mmHg) was somewhat lower than the value reported in freely diving Weddell seals (232 mmHg, Zapol et al., 1989) and the estimated maximum occurred at 3 ATA (Fig. 3A, 20 m), which is similar to measured Pa_{N_2} (Falke et al., 1985). Adjustment of DV_L, and therefore the extent of pulmonary shunt, the exchange capacity of the blood and the pulmonary blood flow influence the magnitude of the maximum and the depth where it occurs. For example, when DV_L was increased to 30 ml kg^{-1}, the peak occurred at 3.8 ATA and was 0.276 ATA (209 mmHg). Once the seal reached the bottom, Pa_{O_2} decayed exponentially throughout the dive and reached 0.045 ATA (34.2 mmHg) immediately before surfacing (Fig. 3A). This value is within the range reported for Pa_{O_2} and PA_{O_2} in the freely diving Weddell seal diving for <17 min (see Fig. 2 in Zapol et al., 1989; and Fig. 3 in Ponganis et al., 1993). However, the predicted Pa_{O_2} is less than the measured end-tidal PA_{O_2} of 70 mmHg after an 11.5 min dive in the Weddell seal but close to the PA_{O_2} of 40 mmHg for dives ranging between 25 and 47 min (Kooyman et al., 1973). Weddell seal dive durations <20 min tend to be deep (200–400 m) while longer dives are often shallow and seldom exceed 130 m (Kooyman et al., 1973). Kooyman et al. (1973) suggested that if alveolar collapse is incomplete during the longer shallower dives but complete during the short deep dives, continued pulmonary gas exchange would reduce O_2 in the lung and explain this counter-intuitive result of a PA_{O_2} that was lower following a long dive (25–47 min) compared with a short one (<20 min). The differences in dive depth used for estimating the data in Fig. 4 compared with those observed in freely diving animals explain why estimated Pa_{O_2} is different from the observed PA_{O_2} after a short dive.

4.3. Changes in blood gases during a dive

The cyclical changes in Pa_{CO_2} and Pv_{CO_2} are not immediately intuitive. During lung compression, the PA_{CO_2} increases resulting in a spike in Pa_{CO_2}. As the arterial blood reaches tissues 22 s later (the arterial transit time), it equilibrates with it. As not all the additional CO_2 is delivered to the tissue, so Pv_{CO_2} increases and reaches a peak which then returns to the lung. This spike keeps recurring with a period that is equal to the transit time but offset in the venous and arterial blood. With each turn of the circulatory system, the relative size of the peak is reduced as a portion of the CO_2 is taken up by the tissues. The height of the initial peak depends on the metabolic rate, the blood flow distribution and $\dot{Q}_{tot}$. When the distribution was adjusted so that 40% of $\dot{Q}_{tot}$ was directed to central circulation, 55% to the muscle, 4% to the brain and 1% to the fat, these changes were significantly dampened and were hardly noticeable. Thus, these cyclical changes are dependent on the tissue

volume and blood flow and will change depending on cardiovascular variation. As the blood flow distribution changes as the animal dives, one would expect to see little variation in Pv_{CO_2} draining from certain tissues while great variation would be observed in others. These changes were also observed for O_2, but as O_2 is consumed at the tissues the height of this spike was less extreme and was only observed for a greater change in blood flow distribution. As period of the peak in venous and arterial P_{CO_2} (and P_{O_2}) is directly related to the transit time and as the arterial and venous values are offset, these cyclical changes could be used to estimate $\dot{Q}_{tot}$. However, these cyclical changes may be dampened in marine mammals by large venous anatomical structures such as the hepatic sinus.

The delay in equilibration of blood gases may explain previous estimates of lung collapse. Falke et al. (1985), sampled arterial blood of freely diving Weddell seals every 30 s during the descent phase of dives. Their results showed that, independent of the maximum dive depth (80–200 m), Pa_{N_2} continued to increase during descent to a depth of 30 m. This was followed by a continual decline in Pa_{N_2} as the animal continued the descent (Falke et al., 1985). It was concluded that this was evidence of alveolar collapse and termination of gas exchange at a depth of 30 m, and the gradual decline in Pa_{N_2} was caused by tissue absorption of the available N_2 in the blood. However, this conclusion is incompatible with cardiopulmonary physiology and rather than evidence of complete alveolar collapse, it suggests a pulmonary shunt that increases with depth (Bostrom et al., 2008). If the data were evidence of alveolar collapse one would expect Pa_{N_2} to immediately approach Pv_{N_2} by the time the alveoli collapse and gas exchange ceased (as seen in Fig. 2). The circulatory transit time (the time for a volume of blood to go from the lung to tissues and back to the lung) was measured at between 2 and 3 min in Weddell seals during forced chamber dives (Kooyman et al., 1972). Thus, 2 min into the dive when the seal reached 30 m, Pv_{N_2} would be close to ambient levels, and if alveoli collapsed this would cause a substantial drop in Pa_{N_2} (similar to the rapid drop in Pa_{N_2} associated with lung collapse during the dive to 305 m, Fig. 2C). The observed Pa_{N_2} in the Weddell seal did not show such a dramatic drop. In fact the Weddell seal data was qualitatively similar to our data in Fig. 2A which initially increased to a maximum and then gradually declined.

During the surface interval following a forced dive, Scholander (1940) reported temporal changes in the respiratory exchange ratio (RER, $\dot{V}_{CO_2} \cdot \dot{V}_{O_2}^{-1}$). The initial RER was <0.7 followed by a gradual increase to values >1.0 which thereafter asymptotically approached values within the theoretically expected range between 0.7 and 1.0. A similar observation was reported in freely diving seals (Kooyman et al., 1973; Boutilier et al., 2001). Kooyman et al. (1973) proposed that these temporal changes represented a rapid uptake of O_2 from depleted haemoglobin and myoglobin with a delay in CO_2 removal as CO_2 and lactic acid is released from the tissue. The model agrees with this suggestion and shows that CO_2 removal lags re-saturation of the O_2 stores by almost 2 min (Fig. 3). Previous studies in freely diving sea lions (Fahlman et al., 2008a,b,c) suggest that an O_2 debt develops during the first dive in a dive bout and this debt is not repaid until the end of the bout. As the gas exchange rate decreases throughout the surface interval it would be most efficient for a diver to exchange O_2 only on the steep portion of the O_2 dissociation curve (Fahlman et al., 2008b). Therefore, diving should resume before the tissues have completely re-saturated with O_2 (Kramer, 1988), and this would maximize the time spent underwater during a foraging bout (Thompson and Fedak, 2001). This results in a gradual accumulation of CO_2 with each subsequent dive, eventually forcing a prolonged surface interval or a period of very short and shallow dives. Consequently, the duration of each dive may be determined by O_2 management while the duration of a bout may be a result of how well CO_2 is handled.

4.4. Adjustment of lung volume and compression (pulmonary shunt)

Kooyman et al. (1972) showed that in forced diving elephant seals, after decompression, Pa_{N_2} remained elevated while the seal was still submerged at 1 ATA (Fig. 5A). Our model suggested that the pulmonary shunt would be between 9% and 14% upon reaching 1 ATA, but this level of shunt resulted in predicted Pa_{N_2} that was significantly lower than the observed Pa_{N_2} (Fig. 5A). Kooyman et al (1972) reported that seals appeared to exhale on occasion, which would increase the shunt while submerged at 1 ATA. To test this, we ran the model by forcing the shunt to be 80% during the decompression phase and while submerged at 1 ATA. Predicted Pa_{N_2} from this attempt agreed well with the observed data, suggesting that the seal may indeed have exhaled during the dive.

One elephant seal that dove with an unusually large DV_{Ao} showed an increasing Pv_{N_2} with dive depth (see Fig. 3 in Kooyman et al., 1972). This is further evidence that the lungs do not collapse at a constant depth but that gas exchange is affected by DV_{Ao} providing diving marine mammals with a behavioural mechanism to adjust collapse depth. Bostrom et al. (2008) suggested that the collapse depth decreases linearly with a decrease in DV_{Ao}, although their analysis did not account for changes in lung gas during a dive. The model presented here allowed us to quantify the extent to which gas exchange is affected by these volume changes. Our data showed that end dive Pv_{N_2} decreases with a decreasing $DV_{Ao} \cdot V_D^{-1}$ ratio (Eqs. (8A) and (8B)), verifying that pre-dive exhalation, or partial inhalation, is an efficient mechanism for adjusting gas exchange during diving. The current model also shows that pre-dive exhalation affects end dive P_{N_2} in a non-linear fashion for shallow dives (Fig. 5). The diffusion rate is affected by several variables that change as the pressure is increased and as air is exchanged across the alveoli. Consequently, gas exchange and the level of pulmonary shunt cannot be investigated separately as they are not independent. In addition, DV_{Ao} has a significant effect on the level of the shunt and the rate at which it changes with depth.

Empirical evidence for this suggestion was presented by Kooyman and Sinnett (1982), where they elegantly showed that following the initial increase in pulmonary shunt during descent (compression), the shunt further increased while the animal was held at pressure (see Fig. 1 in their study). The rate of increase in shunt at the bottom was positively correlated with DV_{Ao}. Assuming that the only difference is DV_{Ao}, diving with a larger DV_{Ao} reduces the shunt. The larger DV_{Ao} also results in more O_2 and N_2 in the lung, leading to a higher PA_{N_2} and PA_{O_2} during descent (compression). At the bottom, the lower shunt enhances gas exchange. The higher rate of gas exchange increases absorption of O_2 and N_2, resulting in a rapid increase in the shunt. Previously reported data from harbour seal #4 support this (see Fig. 1 in Kooyman and Sinnett, 1982). When this animal submerged with a larger DV_L, the pulmonary shunt when reaching the bottom was less and the rate of change in pulmonary shunt was larger.

Our model suggests that adjustment of pulmonary volumes is theoretically plausible and fits data collected from captive studies. Several species of marine mammals (e.g. cetaceans, otariid seals) dive on either full or partial inhalation. An inhalation diver, the Antarctic fur seal, has recently been found to exhale during ascent from dives (Hooker et al., 2005). Expansion of the lungs during ascent decreases pulmonary shunt and therefore increases the rate of arterial O_2 uptake (see the increasing rate of decline at ~20 m, Fig. 3). This may lead to a PA_{O_2} that is lower than Pv_{O_2}, resulting in a reversal of O_2 exchange. This has been suggested as one of the reasons for shallow water blackout that is sometimes observed in breath-hold diving humans after dives that severely deplete tissue and blood P_{O_2}. Ascent exhalations reported in fur seals have

been suggested to maintain the pulmonary shunt by maintaining or reducing the $DV_A \cdot V_A^{-1}$ ratio and therefore the PA_{O_2} in the expanding lung (Hooker et al., 2005). By reducing the amount of O_2 that is returned to the lung, Pa_{O_2} may be maintained >10 mmHg, and prevent EEG changes (Elsner et al., 1970; Kerem and Elsner, 1973). These results emphasize the importance of understanding how gas exchange is modified during diving and how diving animals manage gases and pulmonary shunt to enhance performance.

4.5. Comparison with previous models

Previous modeling attempts have assumed that gas exchange cease instantaneously at some pre-determined depth (Ridgway and Howard, 1979; Falke et al., 1985; Stephenson, 2005b; Fahlman et al., 2006; Zimmer and Tyack, 2007), with collapse depth ranging between 30 m for the Weddell seal (Falke et al., 1985) to 70 m for the bottlenose dolphin (Ridgway and Howard, 1979). We have previously shown that instantaneous collapse is unlikely to occur (Bostrom et al., 2008) and we proposed that compression of the alveoli leads to a pulmonary shunt that is related to the pressure and DV_{Ao} similar to the empirical data reported for California sea lion and harbour seal (Kooyman and Sinnett, 1982). In this paper we show that the assumption of instantaneous collapse and the choice of collapse depth significantly alter model output and estimated P_{N_2} levels (Table 3).

For models assuming an all-or-nothing type of lung collapse, end dive Pv_{N_2} increased by 89% when the collapse depth changed from 30 to 70 m for both dive depths (Model B vs. C, Table 3), illustrating the large effect of lung collapse depth on end dive P_{N_2} estimates. For a dive to 70 m without lung collapse, end dive P_{N_2} increased slightly in venous blood and most tissues (Model C vs. D, Table 3). However, counter intuitively, for the dive to 305 m, end dive P_{N_2} decreased for central circulation, brain and mixed venous blood with the deepest collapse depth of 160 m or with no lung collapse at all (Model D and E vs. C, Table 3). This appears to contradict predictions from simple models that show inconsistent results (Ridgway and Howard, 1979; Kooyman and Sinnett, 1982; Falke et al., 1985). While mathematical models only provide a theoretical framework to understand complex physiological problems, we used empirical data to verify our model estimates and our results highlight the value of our integrated modelling approach. In fact, despite continued N_2 uptake when the collapse depth is increased from 70 to 160 m, the removal begins much sooner and thus compensates for the additional N_2 uptake. Although maximum P_{N_2} is much higher at these deeper collapse depths, depending on the blood flow distribution, the washout can be so fast that it is actually more beneficial (in terms of mitigating the risk of decompression sickness) to have functional gas exchange

Variation in end dive P_{N_2} is much greater for changes in lung collapse depth than for the addition of O_2 and CO_2 to the model (Table 3). Accounting for pulmonary shunt therefore appears to be fundamental in the estimation of P_{N_2} levels. Consequently, conclusions from models that attempt to predict blood and tissue gas tensions during breath-hold diving by assuming an all-or-nothing type gas exchange will be heavily influenced by the chosen lung collapse depth and the species studied in terms of its average dive depth.

Estimated P_{N_2} from the current model is consistent with the data and analysis for the bottlenose dolphin that assumed a collapse depth of 70 m (Model A vs. C, Ridgway and Howard, 1979). Our model estimates also confirm the qualitative analysis of Bostrom et al (2008), in that a pulmonary shunt that increases with depth provides an alternative explanation for the data presented in the bottlenose dolphin (Ridgway and Howard, 1979) and the Weddell seal (Falke et al., 1985). Similarly to the empirical data presented by Kooyman and Sinnett (1982) our model estimates suggest that complete collapse does not occur until depth >150 m, even at low DV_{Ao}. As the average dive depths for many diving mammals are shallower than this collapse depth and the deep divers (e.g., elephant seals, Weddell seals, beaked whales) spend a considerable portion of their time transiting this region, gas exchange will resume for a significant portion of a dive. Therefore, we need to re-assess the assumption that diving mammals are protected against decompression sickness. Repeated dives may result in tissue and blood P_{N_2} levels that cause symptomatic bubble formation and may force the diver to end a foraging bout to safely remove excessive N_2 (Fahlman et al., 2007).

This work is intended as a framework to show how gas exchange can vary during diving. Despite several assumptions in our parameter estimates, this mathematical modeling approach has been useful to bridge the gap between studies proposing quite different lung collapse depths. It has also allowed us to quantify the extent that lung collapse affects tissue and blood gas tensions. Our results emphasize our lack of understanding of how pulmonary compression affects gas exchange and we desperately need more experimental data to describe this.

Acknowledgements

Support for this work was made by a grant to AF from the Office of Naval Research (ONR Award No. N00014-07-1-1098). SKH was funded by a Royal Society Dorothy Hodgkin Research Fellowship. B.B. and D.R.J. were supported by a Discovery Grant to D.R.J. Thanks to Dr. Colin Brauner for fruitful discussions. We are grateful to Dr. Gerry Kooyman for kindly sending us the unpublished heart rate data for the elephant seals and for comments on this work. We would also like to thank Drs. Kooyman and Scholander for having laid the foundation for our understanding how gas exchange is affected by pressure.

References

Andrews, R.D., Jones, D.R., Williams, J.D., Thorson, P.H., Oliver, G.W., Costa, D.P., Le Boeuf, B.J., 1997. Heart rates of northern elephant seals diving at sea and resting on the beach. J. Exp. Biol. 200, 2083–2095.

Bostrom, B., Fahlman, A., Jones, D.R., 2008. Tracheal compression delays alveolar collapse during deep diving in marine mammals. Resp. Physiol. Neurobiol. 161, 298–305.

Boutilier, R.G., Reed, J.Z., Fedak, M.A., 2001. Unsteady-state gas exchange and storage in diving marine mammals: the harbor porpoise and gray seal. Am. J. Physiol. 281, R490–R494.

Burns, J.M., 1999. The development of diving behavior in juvenile Weddell seals: pushing physiological limits in order to survive. Can. J. Zool. 77, 737–747.

Clausen, G., Ersland, A., 1969. The respiratory properties of the blood of the bladdernose seal (*Cystophora cristata*). Respir. Physiol. 7, 1–6.

Davis, R.W., Kanatous, S.B., 1999. Convective oxygen transport and tissue oxygen consumption in Weddell seals during aerobic dives. J. Exp. Biol. 202, 1091–1113.

Elsner, R., Hammond, D.D., Parker, H.R., 1970. Circulatory responses to asphyxia in pregnant and fetal animals; a comparative study of Weddell seals and sheep. Yale J. Biol. Med. (Dec–Feb), 202–217.

Fahlman, A., Olszowka, A., Bostrom, B., Jones, D.R., 2006. Deep diving mammals: dive behavior and circulatory adjustments contribute to bends avoidance. Respir. Physiol. Neurobiol. 153, 66–77.

Fahlman, A., Schmidt, A., Jones, D.R., Bostrom, B.L., Handrich, Y., 2007. To what extent does N_2 limit dive performance in king penguins? J. Exp. Biol. 210, 3344–3355.

Fahlman, A., Hastie, G.D., Rosen, D.A.S., Naito, Y., Trites, A.W., 2008a. Buoyancy does not affect diving metabolism during shallow dives in Steller sea lions (*Eumetopias jubatus*). Aquat. Biol. 3, 147–154.

Fahlman, A., Svärd, C., Rosen, D.A.S., Jones, D.R., Trites, A.W., 2008b. Metabolic costs of foraging and the management of O_2 and CO_2 stores in Steller sea lions. J. Exp. Biol. 211, 3573–3580, doi:10.1242/jeb.023655.

Fahlman, A., Wilson, R., Svärd, C., Rosen, D.A.S., Trites, A.W., 2008c. Activity and diving metabolism correlate in Steller sea lion *Eumetopias jubatus*. Aquat. Biol. 2, 75–84.

Falke, K.J., Hill, R.D., Qvist, J., Schneider, R.C., Guppy, M., Liggins, G.C., Hochachka, P.W., Elliot, R.E., Zapol, W.M., 1985. Seal lung collapse during free diving: evidence from arterial nitrogen tensions. Science 229, 556–557.

Farhi, L.E., 1967. Elimination of inert gas by the lung. Respir. Physiol. 3, 1–11.
Gayeski, T.E., Connett, R.J., Honig, C.R., 1987. Minimum intracellular PO for maximum cytochrome turnover in red muscle *in situ*. Am. J. Physiol. 252, H906–H915.
Hooker, S.K., Miller, P.J.O., Johnson, M.P., Cox, O.P., Boyd, I.L., 2005. Ascent exhalations of Antarctic fur seals: a behavioural adaptation for breath-hold diving? Proc. R. Soc. Lond. B 272, 355–363.
Kerem, D.H., Elsner, R., 1973. Cerebral tolerance to asphyxial hypoxia in the harbour seal. Respir. Physiol. 19, 188–200.
Kooyman, G.L., Hammond, D.D., J.P., S., 1970. Bronchograms and tracheograms of seals under pressure. Science 169, 82–84.
Kooyman, G.L., Kerem, D.H., Campbell, W.B., Wright, J.J., 1973. Pulmonary gas exchange in freely diving Weddell seals, *Leptonychotes weddelli*. Respir. Physiol. 17, 283–290.
Kooyman, G.L., Schroeder, J.P., Denison, D.M., Hammond, D.D., Wright, J.J., Bergman, W.P., 1972. Blood nitrogen tensions of seals during simulated deep dives. Am. J. Physiol. 223, 1016–1020.
Kooyman, G.L., Sinnett, E.E., 1982. Pulmonary shunts in Harbor sels and sea lions during simulated dives to depth. Physiol. Zool. 55, 105–111.
Kramer, D.L., 1988. The behavioral ecology of air breathing aquatic animals. Can. J. Zool. 66, 89–94.
Ponganis, P.J., Kooyman, G.L., Castellini, M.A., 1993. Determinants of the aerobic dive limit of weddell seals: analysis of diving metabolic rates, postdive end tidal PO2's, and blood and muscle oxygen stores. Physiol. Zool 66, 732–749.
Ponganis, P.J., Kooyman, G.L., Zornow, M.H., M.A., C., Croll, D.A., 1990. Cardiac output and stroke volume in swimming harbor seals. J. Comp. Physiol. B 160, 473–182.
Qvist, J., Hill, R.D., Schneider, R.C., Falke, K.J., Liggins, G.C., Guppy, M., Elliot, R.L., Hochachka, P.W., Zapol, W.M., 1986. Hemoglobin concentrations and blood gas tensions of free-diving Weddell seals. J. Appl. Physiol. 61, 1560–1569.
Ridgway, S.H., 1968. The bottlenosed dolphin in biomedical research. In: Gay, W.I. (Ed.), Methods of Animal Experimentation, vol. 3. Academic Press, New York, pp. 387–440.
Ridgway, S.H., Howard, R., 1979. Dolphin lung collapse and intramuscular circulation during free diving: evidence from nitrogen washout. Science 206, 1182–1183.
Scholander, P.F., 1940. Experimental investigations on the respiratory function in diving mammals and birds. Hvalråd. Skrift. 22, 1–131.
Stephenson, R., 2005a. Physiological control of diving behaviour in the Weddell seal Leptonychotes weddelli: a model based on cardiorespiratory control theory. J. Exp. Biol. 208, 1971–1991.
Stephenson, R., 2005b. A theoretical analysis of diving performance in the Weddell seal (*Leptonychotes weddelli*). Physiol. Biochem. Zool. 78, 782–800.
Stockard, T.K., Levenson, D.H., Berg, L., Fransioli, J.R., Baranov, E.A., Ponganis, P.J., 2007. Blood oxygen depletion during rest-associated apneas of northern elephant seals (*Mirounga angustirostris*). J. Exp. Biol. 210, 2607–2617.
Tamburrini, M., Romano, M., Giardina, B., di Prisco, G., 1999. The myoglobin of Emperor penguin (*Aptenodytes forsteri*): amino acid sequence and functional adaptation to extreme conditions. Comp. Biochem. Physiol. B 122, 235–240.
Thompson, D., Fedak, M.A., 2001. How long should a dive last? A simple model of foraging decisions by breath-hold divers in a patchy environment. Anim. Behav. 61, 287–296.
Weathersby, P.K., Homer, L.D., 1980. Solubility of inert gases in biological fluids and tissues: a review. Undersea. Biomed. Res. 7, 277–296.
Zapol, W.M., Hill, R.D., Qvist, J., Falke, K.J., Schneider, R.C., Liggins, G.C., Hochachka, P.W., 1989. Arterial oxygen tensions and hemoglobin concentrations of the free diving Antarctic Weddell SEal. In: Paganelli, C.V., Farhi, L.E. (Eds.), Physiological Function in Special Environments. Springer Verlag, Berlin, pp. 109–119.
Zapol, W.M., Liggins, G.C., Schneider, R.C., Qvist, J., Snider, M.T., Creasy, R.K., Hochachka, P.W., 1979. Regional blood flow during simulated diving in the conscious Weddell seal. J. Appl. Physiol. 47, 968–973.
Zimmer, W.M.X., Tyack, P.L., 2007. Repetitive shallow dives pose decompression risk in deep-diving beaked whales. Mar. Mam. Sci. 23, 888–925.